Electromagnetic Non-Destructive Evaluation (XXI)
D. Lesselier and C. Reboud (Eds.)

doi:10.3233/978-1-61499-836-5-229

Reconstruction of Stress Corrosion Cracking Based on a Regularization Method Using Multi-Frequency Eddy Current Signals

Li WANG[a,1] and Zhenmao CHEN[b]
[a] *College of Science, Xi'an University of Posts and Telecommunications, Xi'an, 710121, China*
[b] *State Key Laboratory for Strength and Vibration of Mechanical Structures, Shaanxi Engineering Research Center of NDT and Structural Integrity Evaluation, Xi'an Jiaotong University, Xi'an, 710049, China*

Abstract. Stress corrosion cracking (SCC) is a prolong breakdown phenomena that occurs in several metal materials and may cause catastrophic accidents. Quantitative nondestructive testing of SCC is important in guaranteeing safety and highly efficient operation in large mechanical systems. However, reconstruction of SCC using eddy current testing (ECT) signals remains a problem given the complicated microstructure of SCC and the ill-posedness of the inverse problem. In this study, the relation between crack parameters and multi-frequency ECT signals is investigated; a regularization method that uses multi-frequency ECT signals is used to reduce the ill-posedness of SCC reconstruction. Conclusions are verified with simulated ECT signals from different conductive crack models.

Keywords. Inverse problem, reconstruction, regularization method, eddy current testing, stress corrosion cracking

1. Introduction

Quantitative evaluation of the defect is one of the targets for eddy current testing (ECT). It estimates the defect type, location and size from the measured signals [1-2]. Depth is frequently underestimated in reconstruction of stress corrosion cracking (SCC) by using ECT signals due to the complicated conductive properties of SCC and ill-posedness of the inverse problem [3]. On the problem of SCC reconstruction, it is found that SCC in different environment and materials has different crack conductive properties [4-5]. The electron discharge machining crack models with multiple nonzero conductivity values have been used to numerical simulation of SCC [6-11]. However, as the number of crack conductivity parameters increases, it is more difficult to accurately reconstruct the SCC profile; that is, the ill-posedness of the inverse problem increases. One of the reasons of the ill-posedness for the ECT inverse problem is different defect parameters maybe correspond to similar values for some ECT signals. Therefore, many numerical criteria are added to the source structure or solution space in practical work, thereby identifying a reasonable solution in a certain range or sense.

[1] Corresponding Author, Li Wang, College of Science, Xi'an University of Posts and Telecommunications, Xi'an, 710121, China; E-mail: wl_3691@163.com.

Based on this point, a regularization method using features of multi-frequency ECT signals is used to SCC reconstruction, thereby reducing the ill-posedness from the complicated conductive property in the crack zone and the inverse problem itself in this study.

2. Crack parameters and ECT signals

A series of numerical simulations have been implemented based on FEM–BEM hybrid method to discuss the relations between crack parameters and ECT signals [12]. A plane numerical model of SCC is adopted in this study in view that crack width variation can be nearly equivalent to crack conductivity change for single-frequency ECT signals [13-14]; in this numerical model, width is fixed to a certain value, and crack-shaped parameters only comprise crack depth and length.

The ECT signals are investigated when the crack parameters, including crack length, depth and conductivity, vary. In this study, a plus-point coil (inner side length 4.5 mm, outer side 5.5 mm and height 2.0 mm) are applied as the inspection probe. The detection object is a SUS304 plate that is 10 mm in thickness, 200 mm in length, 100 mm in width and 1.4 MS/m in conductivity. For single-frequency ECT signals used in Figure 1–3, the excitation frequency is 30 kHz and the liftoff is 1.0 mm.

Figure 1 shows that the crack length mainly influences the start and end positions of parallel scanning ECT signals, while it influences the amplitude and phase of these signals to a certain extent.

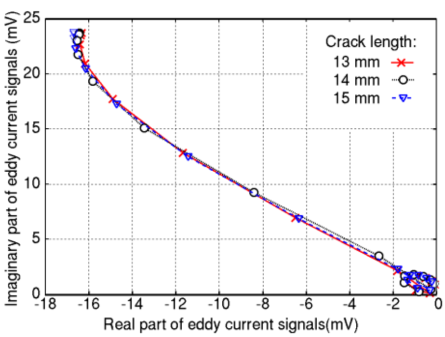

Figure 1. Parallel scanning ECT signals from conductive crack models with different lengths (Crack parameters: depth 3 mm, width 0.4 mm, relative conductivity 3%.)

Figures 2 and 3 demonstrate that the values and distribution of crack conductivity in the depth direction of crack affect the ECT signals in a manner that is similar to the effect of crack depth; this effect is sustained on the amplitude and phase of the ECT signals. Therefore, reconstructing SCC profiles is an ill-posed inverse problem, which is aggravated given the complicated conductivity of SCC in the crack zone. In general, multiple local optimal solutions of crack shape parameters may appear if ECT signals of a single excitation frequency are used when crack shape parameters and conductivity are reconstructed simultaneously.

Certain differences due to various penetration depths occur in the ECT testing for different excitation frequencies when the local conductivity and shape parameters of the crack vary. In particular, high-frequency ECT signals mainly embody information from the crack surface, especially from crack conductivity and length. Low-frequency

ECT signals can express information from the crack depth and crack conductivity from the bottom, as displayed in Figures 4 and 5. Consequently, the features of multi-frequency ECT signals can be used to reconstruct the crack conductivity distribution and depth, thereby solving multiple extreme value problems caused by the complicated conductivity distribution of the SCC to a certain extent.

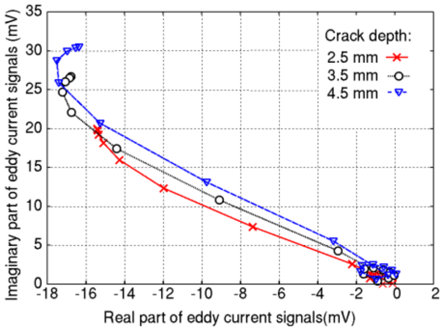

Figure 2. ECT signals from conductive crack models with different depths (Crack parameters: length 14 mm, width 0.4 mm, relative conductivity 3%.)

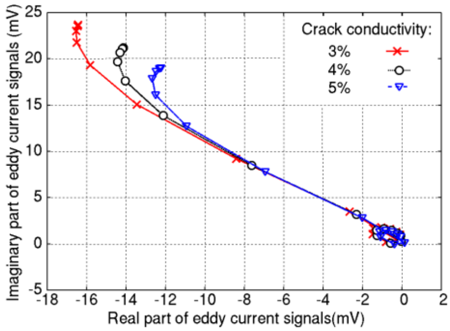

Figure. 3. ECT signals from crack models with different crack conductivities (Crack parameters: length 14 mm, depth 3 mm, width 0.4 mm)

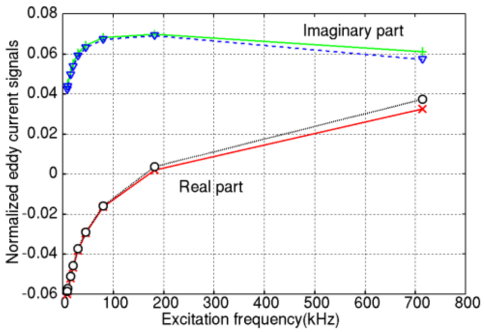

Figure 4. Normalized ECT signals of a scanning point from crack models with the same depth but different conductivity (Solid line is the target signals; the dotted lines with circles or triangles are contrast signals.)

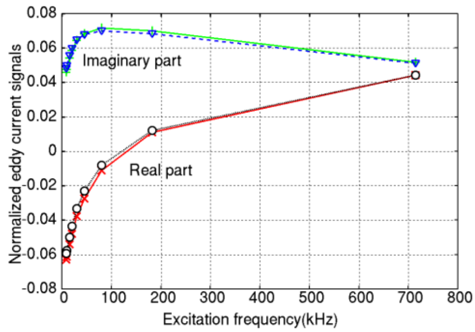

Figure 5. Normalized ECT signals of a scanning point from crack models with the same conductivity but different crack depth (Solid line is the target signals; the dotted lines with circles or triangles are the contrast.)

3. A regularization method using multi-frequency ECT signals

Based on the relation between the crack parameters and features of ECT signals, a regularization method using multi-frequency ECT signals is proposed. The regularization method of crack reconstruction using multi-frequency ECT signals is defined as a series of minimum problems of the mean-squared residual:

$$\min \varepsilon(c,\sigma) = \sum_i \left| Z_{i,j}(c,\sigma) - Z_{i,j}^{obs} \right|^2, \tag{1}$$

where $Z_{i,j}(c,\sigma)$ and $Z_{i,j}^{obs}$ are the calculated and measured signals, respectively. The subscript i represents the ith scanning point, and j represents the jth excitation frequency. Vector c and σ are the crack shape and crack conductivity parameters, correspondingly; vector σ is generally nonzero and needs to be nearly expressed as multiple parameters for the SCC. In general, solving the problem directly is difficult. Alternatively, an optimal solution is gradually approximated by a model-based iterative method; that is, the values of the objective functions will be calculated repeatedly with different crack parameters [15]. However, if the number of iterations or mean-squared error range for optimization (1) is restricted, then several extreme value points may appear and may sometimes be far from the truth; that is, it is usually ill-posed. Moreover, the ill-posedness is aggravated or even does not converge as the number of variables increases.

Thus, the minimal conditions of Formula (1) can be relaxed, and the set of variables that satisfy $\varepsilon(c,\sigma) = \sum_i \left| Z_{i,j}(c,\sigma) - Z_{i,j}^{obs} \right|^2 \le C_j$ is searched, where C_j is the given error bound corresponding to the excitation frequency j. The conductivity value that is near the true value is gradually determined from the crack surface to the bottom by using an excitation frequency from high to low.

The SCC parameters that need to be reconstructed include the crack length, depth, and equivalent conductivity distribution in the crack depth direction. This issue is a high-dimensional optimization problem with multiple parameters. A genetic algorithm is applied to solve the optimization problem.

The basic ideas of the regularization method that uses multi-frequency ECT signals are as follows. First, we aim to find the solution space that satisfies a certain error range for problem (1) and a high excitation frequency. Second, the reconstructed crack length and conductivity values that correspond to the upper layer crack are considered a priori information and thus added to the second optimization problem as the constraints. The current optimal solutions of the second optimization problem are obtained after a number of generations of the genetic algorithm; these solutions correspond to signals of the second excitation frequency. Similarly, the crack length and conductivity results in the second step are considered a priori information and thus added to the next optimization problem as the constraints. Finally, we repeat the same procedure until the termination criterion is satisfied.

The crack conductivity distribution in the depth direction is determined gradually by using the ECT signals of the different excitation frequencies from high to low. The solution scope is reduced by solving the constrained optimization problem successively.

4. Numerical results and discussion

The reconstruction of SCC is performed by considering simulated multi-frequency ECT signals from a 10 mm-thick SUS304 plate as the target signals to validate the proposed strategy. Based on the method described in Section 3, a numerical code that uses a genetic algorithm and a fast-forward solver based on the FEM–BEM hybrid method is developed [16]. For the fast-forward solver, databases of unflawed potentials were established for a search region of 18 mm in length, 5.5 mm in depth and 0.4 mm in width. The search region was subdivided into 198 ($18 \times 11 \times 1$) cells. The target signals are from a conductive elliptical crack model of 14 mm length and 5 mm depth; the crack relative conductivity is 2%, 5%, 8%, 10% and 15% from the surface to bottom of the inspection specimen. Each conductivity value corresponds to thickness 1 mm of the inspection specimen.

To simplify the inversion problem, we only use four parameters to approximately describe the crack conductivity distribution in the reconstruction of SCC. The multi-frequency ECT signals, which correspond to the excitation frequencies of 714, 182, 80, and 30 kHz based on the skin depth of the ECT signals, are used in the objective function, as expressed in Formula (1).

The implementation procedure of SCC reconstruction based on the regularization method and multi-frequency ECT signals is as follows:

First, the signals of a 714 kHz excitation frequency are used in the first objective function $\min \varepsilon(c,\sigma) = \sum_i \left| Z_{i,1}(c,\sigma) - Z_{i,1}^{obs} \right|^2$. A genetic algorithm is used to predict the crack profiles and conductivity distribution. The reconstructed crack length is 14.1 mm, which is from −7.6 mm to 6.5 mm in the crack length direction, after 200 iterations. The conductivity parameters are predicted as 2.51%, 3.22%, 14.43% and 22.24%.

Second, the predicted crack length 14.1 mm and the first conductivity parameter range $\left| \sigma_2 - 2.51\% \right| \le \varepsilon_{11}$ as the constraint conditions are added to the second optimization problem $\min \varepsilon(c,\sigma) = \sum_i \left| Z_{i,2}(c,\sigma) - Z_{i,2}^{obs} \right|^2$, which corresponds to the signals of a 182 kHz excitation frequency, in which ε_{11} is the given error bound.

Similarly, the genetic algorithm is used to solve the constrained optimization problem. The optimal results of the crack conductivity parameters are 2.14%, 4.71%, 7.13% and 23.18%, and the crack depth is 4.5 mm after 300 generations.

Similarly, the crack length 14.1 mm, $|\sigma_1 - 2.14\%| \le \varepsilon_{21}$ and $|\sigma_2 - 4.71\%| \le \varepsilon_{22}$ as the restrained conditions are used for the third objective function which corresponds to the signals of an 80 kHz excitation frequency, where ε_{21} and ε_{22} are the error bounds. The predicted values of the crack conductivity are 1.99%, 5.38%, 6.48%, and 11.29% after 300 generations. The reconstructed depth is 4.7 mm, which corresponds to the true depth of 5.0 mm.

The same procedure is repeated for the constrained optimization problem that corresponds to the signals of a 30 kHz excitation frequency. The reconstructed crack depth that uses the strategy is 4.8 mm. The reconstructed crack conductivity parameters are 1.99%, 5.11%, 6.92%, and 10.39%. Table 1 summarizes the reconstruction results from the regularization method that uses the multi-frequency ECT signals. The above results indicated that the underestimated problem of the SCC depth is solved to a certain extent via the regularization method and multi-frequency ECT signals.

The reconstruction results from the multi-frequency ECT signals with 5% white Gaussian noise via the regularization method are displayed in Table 2. As shown in Figure 6, the reconstruction results of the crack shape parameters via the regularization method are near the truth even for the signals with a 5% white Gaussian noise under the condition that the predicted signals fit well with those in the testing. The results of repeated iterations indicate that the reconstruction results of the crack shape parameters are slightly different due to the randomness of genetic algorithms. However, certain differences are observed in the conductivity distribution of the crack zone, in which it is an equivalent value that is approximately expressed by several conductivity parameters. The different conductivity distributions may correspond to similar ECT signals, which are a difficult point for quantitative SCC. However, the crack conductivity distribution is generally not the key parameter of electromagnetic nondestructive testing. The purpose of reconstructing the crack equivalent conductivity distribution is to obtain crack shape parameters that are near the true values when excitation frequency ranges from high to low. Therefore, the proposed strategy can improve the reconstruction precision of the SCC shape to a certain extent.

Another example is an elliptical crack model with a depth of 4 mm, length of 13 mm and a width of 0.4 mm. The relative conductivity distribution of crack is from 1% to 8% assigned evenly by 8 parameters. According to the minimal mean-squared error, the reconstructed depth is 3.8 mm and the length is 13.2 mm. Reconstruction results from the proposed strategy and the truth are compared in Figure 7 and Table 3. Reconstructions of several other crack models are also conducted. All the results reveal that the scheme is efficient in improving the reconstruction accuracy of SCC.

5. Conclusion

A scheme for the reconstruction of SCC based on the regularization method and multi-frequency ECT signals is used to deal with the ill-posedness from SCC complicated conductive property and the inverse problem. The reconstruction results of the SCC parameters are improved by gradually determining the approximate distribution of the equivalent crack conductivity in the direction of the crack depth. The regularization method reduces the ill-posedness of the problem of SCC reconstruction. Reconstruction with simulated ECT signals from conductive crack models is performed. The results reveal that the proposed strategy effectively improves the precision of SCC reconstruction.

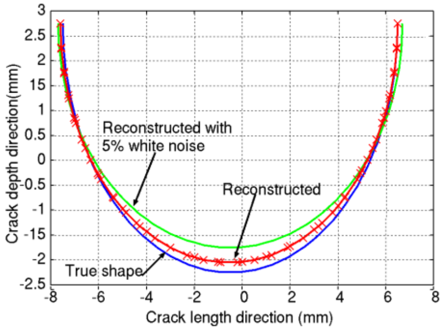

Figure 6. Reconstruction results of crack profiles using simulated ECT signals from an elliptical crack model with the relative conductivity 2%, 5%, 8%, 10% and 15% (with 5% white Gaussian noise)

Table 1. Reconstruction results of an elliptical crack model with the relative conductivity 2%, 5%, 8%, 10% and 15% using multi-frequency ECT signals and the regularization method

Frequency (kHz)	Left edge (mm)	Right edge	Depth (mm)	Crack conductivity parameters (%)			
714	-7.6	6.5	4.2	2.51	3.22	14.43	22.24
182	-7.6	6.5	4.5	2.14	4.71	7.13	23.18
80	-7.6	6.5	4.7	1.99	5.38	6.48	11.29
30	-7.6	6.5	4.8	1.99	5.11	6.92	10.39

Table 2. Reconstruction results of the above elliptical crack model with 5% white Gaussian noise using multi-frequency ECT signals and the regularization method

Frequency (kHz)	Left edge (mm)	Right edge	Depth (mm)	Crack conductivity parameters (%)			
714	-7.7	6.7	2.8	2.51	1.88	7.14	8.59
182	-7.7	6.7	3.9	2.18	4.23	7.32	10.45
80	-7.7	6.7	4.1	2.34	4.04	6.51	9.50
30	-7.7	6.7	4.5	2.50	4.38	6.31	9.30

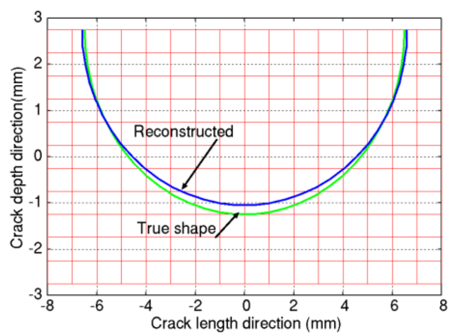

Figure 7. Reconstruction results of crack profiles using simulated ECT signals from a crack model with the crack conductivity from 1% to 8%

Table 3. Reconstruction results of an elliptical crack model with the relative conductivity from 1% to 8% assigned evenly by 8 parameters using multi-frequency ECT signals and the regularization method

Frequency (kHz)	Left edge (mm)	Right edge (mm)	Depth (mm)	Crack conductivity parameters (%)			
714	-6.6	6.6	3.1	1.41	2.98	14.90	9.88
182	-6.6	6.6	3.8	1.65	2.18	8.88	9.93
80	-6.6	6.6	3.8	1.76	2.19	6.73	6.57
30	-6.6	6.6	3.8	1.79	2.23	6.00	6.00

Acknowledgement

This work is supported in part by the Scientific Research Scheme of Education Department of Shaanxi Province (15JK1677), the Natural Science Basic Research Program of Shaanxi (2017JM1015) and the National Magnetic Confinement Fusion Program of China (2013GB113005).

References

[1] B.A. Auld, J.C. Moulder, Review of advances in quantitative eddy current nondestructive evaluation, *J Nondestruct Eval* **18**(1999), 3–36.
[2] S. Norton, J. Bowler, Theory of eddy current inversion, *Journal of Applied Physics* **73**(1993), 501–512.
[3] N. Yusa, H. Huang, K. Miya, Numerical evaluation of the ill-posedness of eddy current problems to size cracks, *NDT & E International* **40** (2007), 185–191.
[4] T Huang, D Zhang, Z Chen, A study on the distribution of conductivity of a stress corrosion crack based on ECT, *J Measurement Tech.* **24**(2010), 58–61.
[5] H. Huang, N. Yusa, K. Miya, H. Hashizume, T. Sera, S. Hirano, Electromagnetic modeling of Stress Corrosion Cracks in Inconel welds, *E-Journal of Advanced Maintenance*, **2**(2010/2011), 168–180.
[6] Z. Chen, L. Janousek, N. Yusa, K. Miya, A nondestructive strategy for the distinction of natural fatigue and stress corrosion cracks based on signals from eddy current testing, *ASME J Pressure Vessel Technology*, **219**(2007), 719–728.
[7] N. Yusa, H. Shishido, H. Hashizume, Evaluating the iII-posedness of inverse problem to size flaws from eddy current NDT signals obtained with an absolute type probe, *Applied Mechanics & Materials*, **619**(2014), 337–341.
[8] L. Wang, Z. Chen, A multi-frequency strategy for reconstruction of deep stress corrosion cracks from ECT signals of multiple liftoffs, *Int J Appl Electromagn Mech.*, **33**(2010), 1017–1023.
[9] Z Chen, M Rebican, N Yusa, K Miya, Fast simulation of ECT signal due to a conductive crack of arbitrary width, *IEEE Transactions on Magnetics*, **42**(2006), 683–686.
[10] F Kojima, N Kubota, K Kobayashi, T Takagi, Shape recovery of natural crack using evolutionary programming related to eddy current testing, *Int J Appl Electromagn Mech.* **15**(2001), 243–247.
[11] N Yusa, Z Chen, K Miya, T Uchimoto, T Takagi, Large-scale parallel computation for the reconstruction of natural stress corrosion cracks from eddy current testing signals, *NDT & E International* **36**(2003), 449–459.
[12] F. Matsuoka, *Calculation of 3-D eddy current by the FEM-BEM coupling method*, Proc. of the IUTAM, North-Holland, 1986.
[13] N. Yusa, K. Miya, Discussion on the equivalent conductivity and resistance of stress corrosion cracks in eddy current simulations, *NDT & E Int.*, **42**(2009), 9–15.
[14] N Yusa, S Perrin, K Mizuno, et al. Numerical modeling of general cracks from the viewpoint of eddy current simulations, *Ndt & E International*, **40**(2007), 577–583.
[15] Y. Li, L. Udpa, S. Udpa, Three-dimensional defect reconstruction from eddy-current signal by using a genetic local search algorithm, *IEEE Trans. Magn.*, **40**(2004), 410–417.
[16] Z Chen, K Miya, ECT inversion using knowledge based forward solver, *J Nondestruct Eval.*, **17** (1998), 167–175.